Chalcogenide Letters Vol. 13, No. 8, August 2016, p. 351 - 357

MORPHOLOGICAL EVOLUTION OF MoS_2 NANOSHEETS BY CHEMICAL VAPOR DEPOSITION

X. WANG, Y. P. ZHANG*, Z. Q. CHEN
Faculty of Materials and Energy, Southwest University, Chongqing 400715, China

MoS_2 nanosheets are synthesized using a low-pressure chemical vapor deposition (CVD) system at elevated temperature on Si substrates with S and MoO_3 power as its precursors. SEM and XRD measurements indicate that the morphology and structure of the deposited MoS_2 nanosheets are highly dependent on the spatial location of silicon substrate, with the preferred crystalline orientation varied from (108) to (201) as the sample further from the sulphur source. XPS shows that the MoO_2 constituent increases slightly as the distance further away from the sulphur source. The nanostructured MoS_2 film exhibits strong photoluminescence in the visible range. This paper may provide new insight into our understanding the kinetic dynamics related to the MoS_2 growth.

(Received June 11, 2016; Accepted August 17, 2016)

Keywords: Transition Metal Dichalcogenides, MoS_2, Nanosheets, Chemical Vapor Deposition

1. Introduction

Layered materials have attracted extensive attention and found promising applications for sensors, catalysis, and energy storage because of their unique structure with high epecific surface area and exotic physical and chemical properties.[1-2] Besides the zero-bandgap graphene, transition metal dichalcogenides (TMDs) and transition metal oxides (TMOs) are two important materials with the two-dimensional layered structure.[3-4] Researchers have made every endeavors in developing reliable and flexible approaches for obtaining thin layer MoS_2, and explored a variety of techniques in synthesizing MoS_2 nanosheets, such as exfoliation,[5-6] hydrothermal synthesis,[7] physical vapor deposition (PVD) and chemical vapor deposition (CVD). [8-13] Among these methods, chemical vapor deposition has been one of the most promising methods of producing large-area and high-quality MoS_2 thin films and nanomaterials. The precursors and deposition parameters used in CVD have great affects on the structural mophology of MoS_2 nanosheets. Bulk MoS_2 has an indirect bandgap of 1.2 eV, but for layered MoS_2, its bandgap increases as the layer number decreases, and the monolayer MoS_2 has a direct bandgap of 1.9 eV.[1-4] Besides bulk and monolayer MoS_2, nanoscale MoS_2 has ample property variations by tuning the structural changes and find new potential applications. Therefore, it is of great importance to achieve the controlled growth of MoS_2 nanosheets and get deeper insight into the reaction mechanism since the process is complex and related to many factors.

In this paper, we report the effect of the substrate positions on the structural mophologies of MoS_2 nanosheets in a CVD system. Large-area of MoS_2 nanosheets were obtained using low-pressure CVD with the precursors of sulphur and MoO_3 powder and characterized by field-emission scanning electron microscopy (SEM), X-ray diffraction (XRD), X-ray photoelectron spectroscopy (XPS), Photoluminescence (PL) and Raman spectroscopy.

*Corresponding author: zhangyyping@yahoo.com

2. Experimental methods

The experimental setup for the synthesis of MoS_2 nanosheets are illustrated in Fig. 1. The quartz tube with smaller diameter (D=20 mm) was used to ensure sufficient reaction of the vapor of S and MoO_3. Two grams of sulphur powder was put in a ceramic boat and placed at the inlet of CVD furnance 30 cm away from the center, while 50 mg of MoO_3 powder was put in another ceramic boat and located at the centre of furnance. The cleaned four Si substrates (sonication in acetone, alcohol for 10 min each and subsequent dried by air-blow) were faced up and placed at different position in the small quartz tube. The insulating plug placed between the MoO_3 and the sulfur can prevent S powder from evaporating too quickly. During the synthesis of MoS_2 nanosheets, the temperature of the reaction chamber was slowly heated to 750℃ (20℃/min) and kept for 60 min and then the furnace was naturally cooled down to room temperature. The process was carried with an argon environment (100 sccm) at a chamber pressure of 100 Pa.

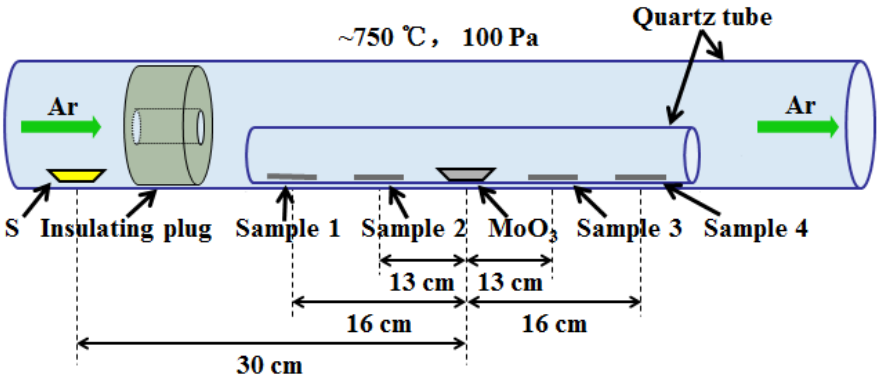

Fig. 1. Schematic illustration of low-pressure CVD system and the sample position.

The structural mophology of resulting products was observed using field-emission scanning electron microscopy (FESEM) (JMS-7800F, JEOL Ltd, Japan) and X-ray diffraction (XRD) (XRD-7000, Shimadzu). The chemical composition and oxidation state were studied using X-ray photoeletron spectroscopy (XPS) (ESCALAB250Xi, ThermoFisher Ltd). The pass energy for survey scan is 100 eV, and for Mo 3d and S 2p is 20 eV. The Raman and PL spectra were obtained by using a Renishaw inVia 2000 micro-Raman system at room temperature in an ambient air. The excitation laser line is 532 nm.

3. Results and discussion

Figure 2 shows the SEM images of MoS_2 nanosheets deposited on the Si(100) substrates located at different positions. The deposited material, as shown in Fig. 2(a)-(d), is composed of numerous densely grown, well-faceted, well-distributed, semi-vertically and interleaving lamellar nanosheets with rough edges. As the distance from the sulphur source increases, the thicknesses of MoS_2 nanosheets gradually decrease from 100-200 nm to 40-60 nm and the lateral sizes from around 6 μm to 1μm. The surface edges become rougher with sample further from the sulphur source. As the insertion shown in Fig. 2(a), the deposition of MoS_2 nanosheets is continuous on the entire Si surface (1 cm^2) which shows a high material yield and a controllable nanosheet morphology.

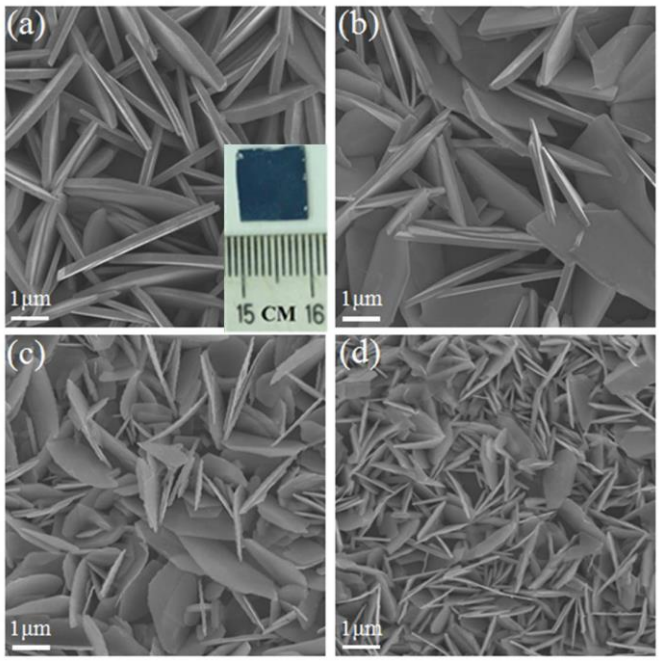

Fig. 2.The SEM images of the MoS_2 nanosheets of 4 samples placed at different positions. (a) Sample 1, (b) Sample 2, (c) Sample 3, and (d) Sample 4 .

XRD was employed to characterize the lattice structure of rusulting products, which is shown in Fig. 3. Figure 3(a) shows the patterns of MoS_2 nanosheets in the range of 10-80°. Because the the peak intensities differed too widely, Figure 3(b) and (c) give the enlarged diffraction peaks in the range of 10° to 65° and 65° to 75°, respectively. The XRD patterns show that the samples are mainly composed of MoS_2 and a small amount of MoO_2 crystals. The diffraction peaks (2θ) positioned at 14.5°, 68.8°, 69.4°, and 69.7° are ascribed to the lattice planes (002), (200), (108) and (201) of the crystalline 2H-MoS_2 (JCPDS card no.75-1539).[14] The peaks (2θ) at 18.5°, 26.1°, 37.4°, and 57.6° are attributed to the lattice planes (100), (110), (111), and (300) of MoO_2 (JCPDS card no.76-1807). As the distance of the samples from the sulphur source increases, the peak intensity for MoO_2(111) increases slightly. Meanwhile, the peak for MoS_2(108) decreases, and the peak for MoS_2(201) increases as the distance from sulphur source increases.

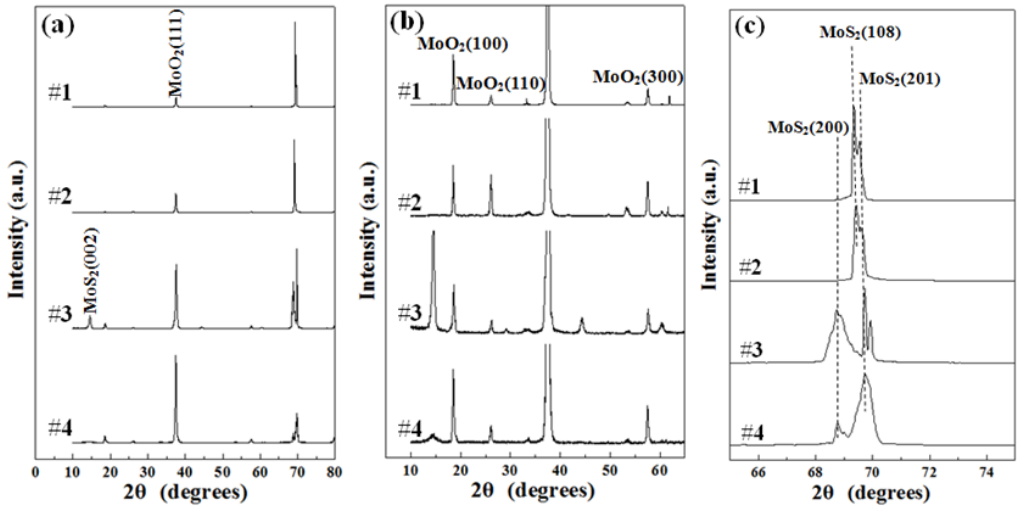

Fig. 3. XRD patterns of the MoS_2 nanosheets for Samples 1-4 for the diffraction angle (2θ) in the range of (a) 10-80°, (b) 10-65°, and (c) 65-75°.

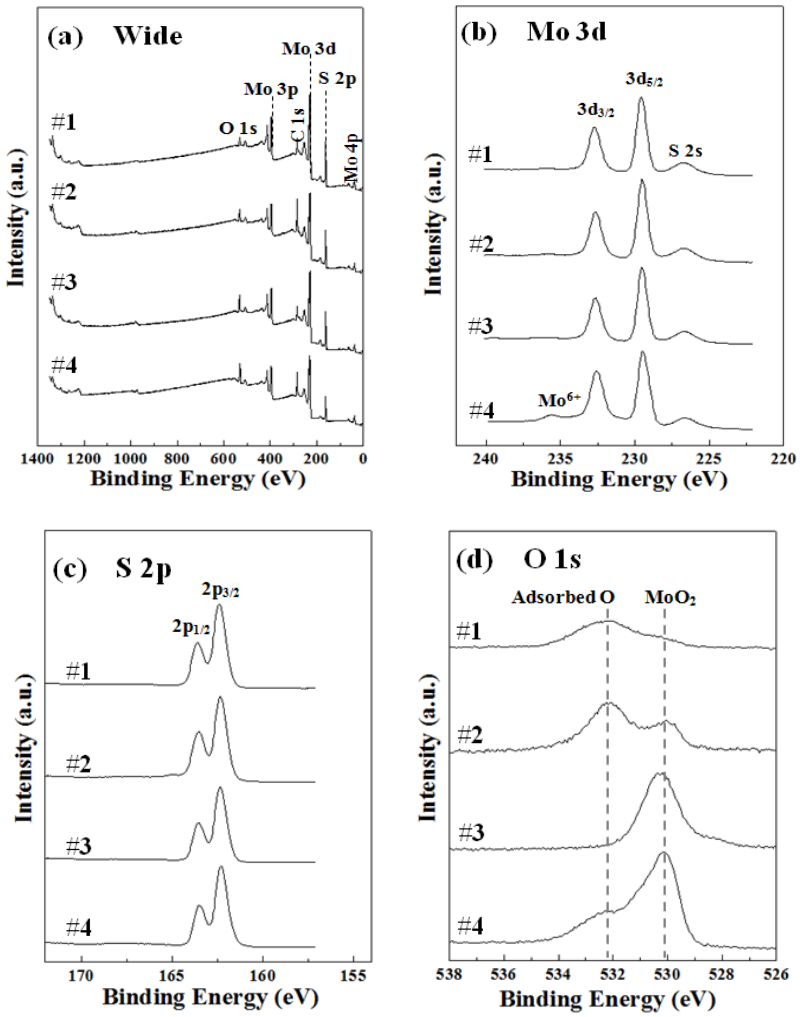

Fig. 4. XPS spectra of the MoS_2 nanosheets of Sample 1-4. (a) survey scan, and the spectra of (b) Mo 3d, (c) S 2p and (d) O 1s.

XPS is a powful technique to provide the composition of the surface region, and distinguishes the different chemical states of one element. Figure 4 shows the XPS spectra of the four samples placed at different positions. The survey scan in Fig. 4(a) only shows the peaks derived from the elements of Mo, S, O, and C. The C 1s signal represents the adventitious carbon. The ratio of O/Mo increases as the distance of samples from sulphur source increases, which is consistent with the XRD results. The Mo 3d spectra are shown in Fig. 4(b), in which the small peaks at binding energy of 226.7 eV are due to the electrons of S 2s corresponding to MoS_2.[15-16] The peak at 235.8 eV of Mo $3d_{3/2}$ for Sample 4 is ascribed to the existence of Mo-O bond of Mo^{6+}, it is due to the distance of sample 4 from the sulfur source is the greatest and surface oxidation. The main peaks at binding energy of 229.5 eV and 232.6 eV are attributed to Mo 3d doublet peaks of $3d_{5/2}$ and $3d_{3/2}$ which are consistent with Mo^{4+} in MoS_2.[15-16] Additionally, the peaks at 162.3 eV and 163.5 eV in the S 2p spectra in Fig. 4(c) are ascribed to S 2p doublets of $2p_{3/2}$ and $2p_{1/2}$. In Fig. 4(d), the O 1s core level spectra of the four samples, the weak peaks located at 532.2 eV presence in a very small portion which is most likely related to physically adsorbed oxygen molecules. The peaks at the bingding energy of 530.1 eV are caused by O^{2-} oxidation state in MoO_2, meanwhile, as the distance of the samples from the sulphur source increases, the peak intensity for O 1s expect adsorbed O increases slightly. Moreover, if the sensitive factors for Mo 3d and S 2p are selected as 2.867 and 0.57, respectively, the calculated stoichiometric ratio of S/Mo is approximately 1.76, which is comparable to the reported values.[17-18]

In the chemical vapor reaction process, MoO_3 presumably changes to MoO_2 at the sulphur envrionment. Afterwards, MoO_2 is further sulphurized to MoS_2 by reacting with the sulphur vapor.[18] Our experiments show the morphology and composition of the resulting MoS_2 nanosheets are related to the S/Mo atomic ration in the reaction atomsphere. As the sample positioned further to the sulphur source, the MoO_2 constituent increases slightly. The sulphur vapor concentration alone the small quatz tube drops as the sample distance further from the sulphur source. Therefore, the MoO_2 in Sample 1 is fully sulphurized into MoS_2, while the MoO_2 in Sample 4 is only partially sulphurized.

These MoS_2 nanosheets were further characterized by Raman spectroscopy and photoluminescence (PL), shown in Fig. 5. In Raman spectra, both A_{1g} and E^1_{2g} vibrational modes are associated with out-of-plane vibration of sulfur atoms and in-plane vibration of Mo and S atoms, respectively.[19] The fitting results for Raman spectra in Fig. 5(a) show that these two modes are located at 382 and 407 cm^{-1} for the 2H-MoS_2 nanosheets in Sample 1, and the frequency difference is about 25 cm^{-1} which is confirmed by XRD measurements as well. As for Sample 2, these two modes are located at 384 and 406 cm^{-1}, respectively, and the frequency difference is about 22 cm^{-1}. The frequency difference between the two prominent Raman modes (A_{1g} and E^1_{2g}) has been known closely related with the layer number of MoS_2, therefore, our Raman resultes indicating the nanosheets consists of many MoS_2 layers stacked together. The peak at 365 cm^{-1} is attributed to the stretching vibration of molybdyl (Mo=O),[20] and its intensity is stronger than that of Sample 1. That is consistent with the results of XPS.

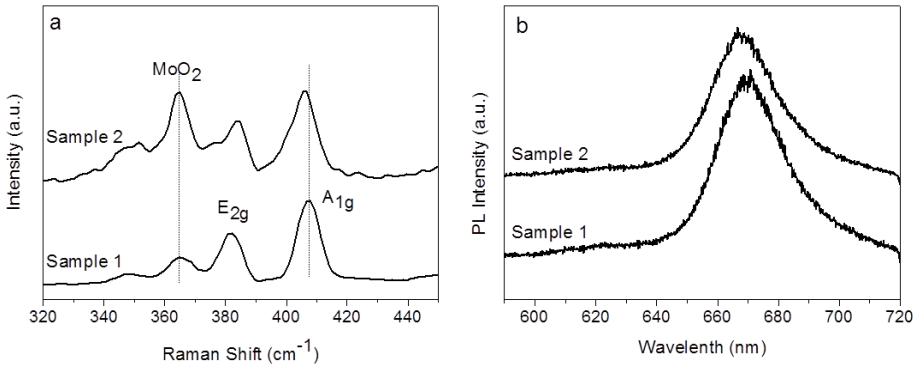

Fig. 5. Raman (a) and Photoluminescence (b) spectra of the MoS_2 nanosheets of the two samples placed at different positions.

PL spectra for the MoS_2 nanosheets are shown in Fig. 5(b), in which a distinct peak at 671 nm (1.85 eV) is observed. Compared with Sample 1, the PL peak for Sample 2 is about 667 nm.The PL intensity could depend on many parameters such as height, strain, thickness, the number of layers and defects of nanosheets. It has been reported that the indirect gap bulk MoS_2 and MoS_2 nanosheets with thickness greater than 5 nm do not exhibit photoluminescence.[21] Surprisingly, the as-synthesized MoS_2 nanosheets still exhibit PL signal though their thickness are about 100 nm from the SEM observarion. The PL intensity could depend on many parameters including thickness, strain, defects, and height of nanosheets. The thickness of the synthesized MoS_2 nanosheets is about 100 nm from the SEM observation, and surprisingly these nanosheets still exhibit PL signal. The observed PL signal for thick nanosheets may be due to the structural discontinuity at the nanosheet edges, which induces variation of the electronic structure of MoS_2 nanosheets.[22]

4. Conclusions

Large-area MoS_2 nanosheets were successfully synthesized by low-pressure CVD using sulphur and MoO_3 powder as precursors at elevated temperature. The whole sample was covered with high-quality crystalline MoS_2 nanosheets and the stoichiometric ratio of MoS_2. The further

the distance of sample from the sulphur source, the smaller the width and size of the MoS_2 nanosheets. As the distance from sulphur inceases, the preferred crystalline orientation changes to (210) from (108), and the MoO_2 constituent increases slightly. The nanostructured MoS_2 film exhibits strong photoluminescence in the visible range due to its sharp edges. This paper may provide new insight into our understanding the kinetic dynamics on MoS_2 growth.

Acknowledgement

Project supported by the National Natural Sience Foundation of China (Grant No. 21173170) and the Fundamental Research Funds for the Central Universites, China (Grant No. XDJK2015D001).

References

[1] B. Radisavljevic, A. Radenovic, J. Brivio, et al. Nat. Nanotechnol. **6**, 147 (2011).
[2] K. F. Mak, C. G. Lee, J. Hone, et al, Phys. Rev. Lett. **105**, 136805 (2010).
[3] Q. H. Wang, K. Kalantar-Zadeh, A. Kis, et al. Nat. Nanotechnol. **7**, 699 (2012).
[4] Y. H. Lee, X. Q. Zhang, W. J. Zhang, et al. Adv. Mater. **24**, 2320 (2012).
[5] J. N. Coleman, M. Lotya, A. O'Neill, et al. Science **331**, 568 (2011).
[6] R. J. Smith, P. J. King, M. Lotya, et al. Adv. Mater. **23**, 3944 (2011).
[7] L. J. Ye, H. Y. Xu, D. K. Zhang, et al. Mater. Res. Bull. **55**, 221 (2014).
[8] H. Liu, M. W. Si, S. Najmaei, et al. Nano Lett. **13**, 2640 (2013).
[9] X. S. Wang, H. B. Feng, Y. M. Wu, et al. J. Am. Chem. Soc. **135,** 5304 (2013).
[10] Y. J. Zhan, Z. Liu, S. Najmaei, et al. Small **8**, 966 (2012).
[11] Y. F. Yu, C. Li, Y. Liu, et al. Sci. Rep. **3**, 1866 (2013).
[12] J. Mann, Q. Ma, P. M. Odenthal, et al. Adv. Mater. **26**, 1399 (2014).
[13] X. Ling, Y. H. Lee, Y. X. Lin, et al. Nano Lett. **14**, 464 (2014).
[14] W. X. Gu, J. Y. Shen, X. Y. Ma, Nanoscale Res. Lett. **9**, 100 (2014).
[15] B. Cho, A. R. Kim, Y. Park, et al. ACS Appl. Mater. Interfaces **7**, 2952 (2015).
[16] S. McDonnell, R. Addou, C. Buie, et al. ACS Nano **3**, 2880 (2014).
[17] H. T. Lin, X. Y. Chen, H. L. Li, et al. Mater. Lett. **64**, 1748 (2010).
[18] D. Q. Gao, M. S. Si, J. Y. Li, et al. Nanoscale Res. Lett. **8**, 129 (2013).
[19] X. L. Li, Y. D. Li, Chem. Eur. J. **9**, 2726 (2003).
[20] X. Ling, Y. H. Lee, Y. Lin, et al. Nano Lett. **14**, 464 (2014).
[21] G. Eda, H. Yamaguchi, D. Voiry, et al. Nano Lett. **11**, 5111 (2011).
[22] G. Deokar, D. Vignaud, R. Arenal, P. Louette, J. F. Colomer, Nanotechnology **27,** 075604 (2016).